Z. anorg. allg. Chem. **553** (1987) 163—171 J. A. Barth, Leipzig

Ordered Magnetic Frustration. XI [1—10]

Refinement of the Crystal and Frustrated Magnetic Structures of the Direct Weberite Na_2NiCrF_7 by Neutron Powder Diffraction

Y. LALIGANT, G. FEREY*

Le Mans (France), Laboratoire des Fluorures (UA CNRS 449), Faculté des Sciences Université du Maine

G. HEGER[1])

Karlsruhe, Kernforschungs-Zentrum Karlsruhe

J. PANNETIER

Grenoble (France), Institut Laue-Langevin

Dedicated to Professor Rudolf Hoppe on his 65th Birthday

Abstract. The nuclear and magnetic structures of the ferrimagnetic ($T_c = 4$ K) weberite Na_2NiCrF_7 were solved by neutron powder diffraction experiments at $T > 4$ K, 2.13 and 1.5 K respectively. The cell is orthorhombic (Space group Imma, a = 7.183(1) Å, b = 10.224(1) Å, c = 7.414(1) Å, Z = 4). The nuclear and the magnetic cells are identical. An anomaly in the thermal variation of the intensity of some magnetic reflections at 2 K is due to the disparity between the thermal variation of the magnetization of the two sublattices of Ni^{2+} and Cr^{3+}. The former is already close to its maximum value at 2 K ($\mu_{Ni^{2+}} = 1.65(2)\,\mu B$ at 2.13 K and 1.75(2) μB at 1.5 K) whereas the latter continues to increase below this temperature ($\mu_{Cr^{3+}} = 1.84(5)\,\mu B$ at 2.13 K and 2.22(6) μB at 1.5 K.)

Geordnete magnetische Erstarrung. XI. Verfeinerung der Kristallstruktur und der erstarrten magnetischen Strukturen von Weberit Na_2NiCrF_7 durch Neutronen-Pulverdiffraktionsmessung

Inhaltsübersicht. Die Gitter- und magnetische Strukturen des ferrimagnetischen ($T_c = 4$ K) Weberit Na_2NiCrF_7 wurden durch Neutronen-Pulverdiffraktionsexperimente bei $T > 4$ K, 2,13 K bzw. 1,5 K aufgeklärt. Die Zelle ist orthorhombisch (Raumgruppe Imma, a = 7,183(1) Å, b = 10,224(1) Å, c = 7,414(1) Å, Z = 4). Die Gitter- und magnetischen Zellen sind identisch. Eine Anomalie in der thermischen Veränderung der Intensität einiger magnetischer Reflexe bei 2 K beruht auf der Ungleichheit zwischen der thermischen Veränderung der Magnetisierung der Untergitter

[1]) Present address: Laboratoire Léon Brillouin, C.E.N. Saclay, F91191 Gif/Yvette

von Ni^{2+} und Cr^{3+}. Während die Magnetisierung im ersten Fall bei 2 K schon nahe an ihrem maximalen Wert ist ($\mu_{Ni}{}^{2+} = 1{,}65(2)$ μB bei 2,13 K und 1,75(2) μB bei 1,5 K) steigt sie im letzten Falle noch kontinuierlich unterhalb dieser Temperatur an ($\mu_{Cr}{}^{3+} = 1{,}84(5)$ μB bei 2,13 K und 2,22(6) μB bei 1,5 K).

Introduction

The concept of ordered magnetic frustration that we have developed over the years [1—10] describes the various arrangements adopted by spins in antiferromagnetic interaction when the corresponding cations form a triangular network. This geometry is encountered in $Na_2M^{2+}M^{3+}F_7$ compounds with the weberite structure [7, 11—14]. We recently solved the ambiguity concerning the true space group of the weberite [7] which was claimed to be either Imma [12] (h+k+l=2n and hk0: h = 2n) or Imm2 [11, 13, 14] (h+k+l = 2n) by different authors. We showed that the weak reflections hk0 with h = 2n+1 which caused some authors to describe the weberite in Imm2 were only due to Renninger effect, and are therefore, not intrinsic to the structure.

This crystallographic problem being solved, we refined the true magnetic structure of Na_2NiFeF_7 [15,7] which corresponds to a complete frustration of the antiferromagnetic superexchange coupling of Ni^{2+}. Indeed, Ni^{2+} spins adopt a parallel arrangement and are coupled antiferromagnetically to Fe^{3+} spins. The superexchange coupling Fe^{3+}—Ni^{2+} governs the magnetic structure and it was thought interesting to compare the case in which the interaction M^{3+}—Ni^{2+} is weak in order to see the evolution within the same structure of the frustrated magnetic character with the disparity of superexchange interactions. This case occurs with Na_2NiCrF_7 [16]. We report here its crystal and magnetic structures.

Experimental

Powder samples of Na_2NiCrF_7 were obtained by heating a stoichiometric mixture of elementary fluorides in sealed gold tubes at 700°C for 48 hours. The anomaly observed by a preliminary neutron thermo-diffractometry experiment at 2 K [17] lead us to study the magnetic structure of Na_2NiCrF_7 and its thermal variation. Neutron diffraction patterns were collected on the D1B powder diffractometer at the Institut Laue-Langevin (Grenoble) using the wavelength $\lambda = 2.529$ Å. The green sample was contained in a cylindrical vanadium can ($\varnothing = 10$ mm) held in a vanadium-tailed liquid helium cryostat.

Diffraction patterns ($4° < 2\Theta < 84°$ in steps of 0.02°) were collected at constant temperature every 0.10 K in the range 1.5—6 K. As previously observed [16], the compound becomes ferrimagnetic on cooling below 4 K. The patterns collected above this temperature were summed to refine the nuclear structure.

Two other diffraction patterns at 2.13 and 1.5 K were recorded to determine the two magnetic structures which may exist in the temperature ranges 1.5—2 K and 2—4 K, respectively.

The data were analysed by the RIETVELD method [18] as modified by HEWAT [19]. The nuclear scattering lengths and magnetic form factors were taken from [20] and [21] respectively. The peak shape does not deviate from a gaussian profile. So, integrated intensities were determined from the thermodiffractograms by fitting the shape of the Bragg peaks to Gaussians using the INTEGR program [22]. The magnetic models were deduced from the BERTAUT's theory [23].

Results

1. Nuclear structure

The nuclear structure has been refined at $T > 4$ K using 16 peaks corresponding to 28 (hkl) triplets. The final values of the cell parameters and atomic coordinates were given in Table 1. The isotropic thermal parameters were fixed to 1.0, 0.56, and 0.20 $Å^2$ respectively for sodium, fluorine and metals. The corresponding distances appear in Table 2 and are in good agreement with usual Ni—F and Cr—F values [24]. The crystal chemistry of the weberite structure is well

Table 1 Refined cell parameters (Å) and atomic coordinates at $T > 4$ K
Standard deviations are given in parentheses
a = 7.183(1) Å b = 10.224(1) Å c = 7.414(1) Å

Atom	x	y	z	B
Na1	0	0	0	1.0
Na2	1/4	1/4	3/4	1.0
F1	0	1/4	0.144(1)	0.56
F2	0	0.4120(6)	0.7265(9)	0.56
F3	0.1957(6)	0.3850(4)	0.4361(7)	0.56
Ni^{2+}	1/4	1/4	1/4	0.20
Cr^{3+}	0	0	1/2	0.20

$R_p = 0.047$ $R_{wp} = 0.048$ $R_{nucl} = 0.028$

Table 2 Interatomic distances (Å) and angles (°) in Na_2NiCrF_7 at $T > 4$ K
Standard deviations are given in parentheses

Ni^{2+} octahedron					
Ni—F1	2×	1.960(3)	F1—F1		3.920(4)
Ni—F3	4×	1.984(5)	F1—F3	4×	2.927(7)
<Ni—F>		1.976 ($D_{SHANNON}$ [24] = 1.975)		4×	2.643(5)
			F3—F3	2×	2.761(6)
				2×	2.868(7)
Cr^{3+} octahedron					
Cr—F2	2×	1.903(6)	F2—F2		3.805(9)
Cr—F3	4×	1.901(4)	F2—F3	4×	2.591(7)
<Cr—F>		1.902 ($D_{SHANNON}$ [24] = 1.900)		4×	2.785(6)
			F3—F3	2×	2.540(6)
				2×	2.830(6)
Superexchange angles and metal-metal distances					
Ni—Ni	2×	3.592(3)	Ni—F1—Ni		132.8(2)
Ni—Cr	4×	3.632(3)	Ni—F3—Cr		138.6(2)
Sodium polyhedra					
Na1—F1	2×	2.770(3)	Na2—F2	4×	2.445(3)
Na1—F2	2×	2.226(6)	Na2—F3	4×	2.738(5)
Na1—F3	4×	2.520(4)			

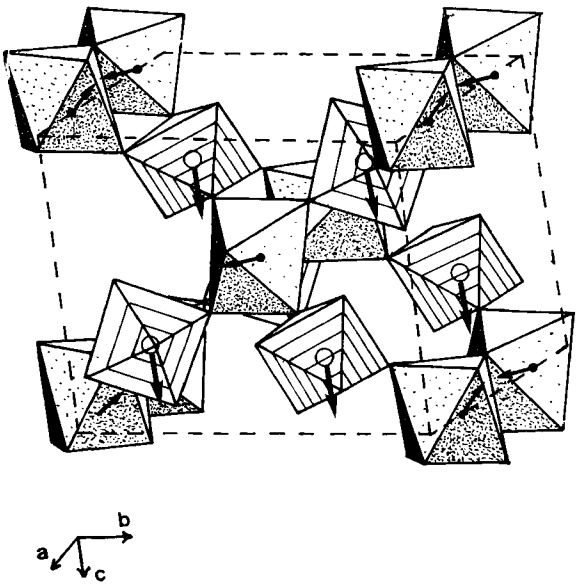

Fig. 1 Perspective view of the weberite structure. M^{2+} and M^{3+} octahedra are dot-shaded and hatched respectively.

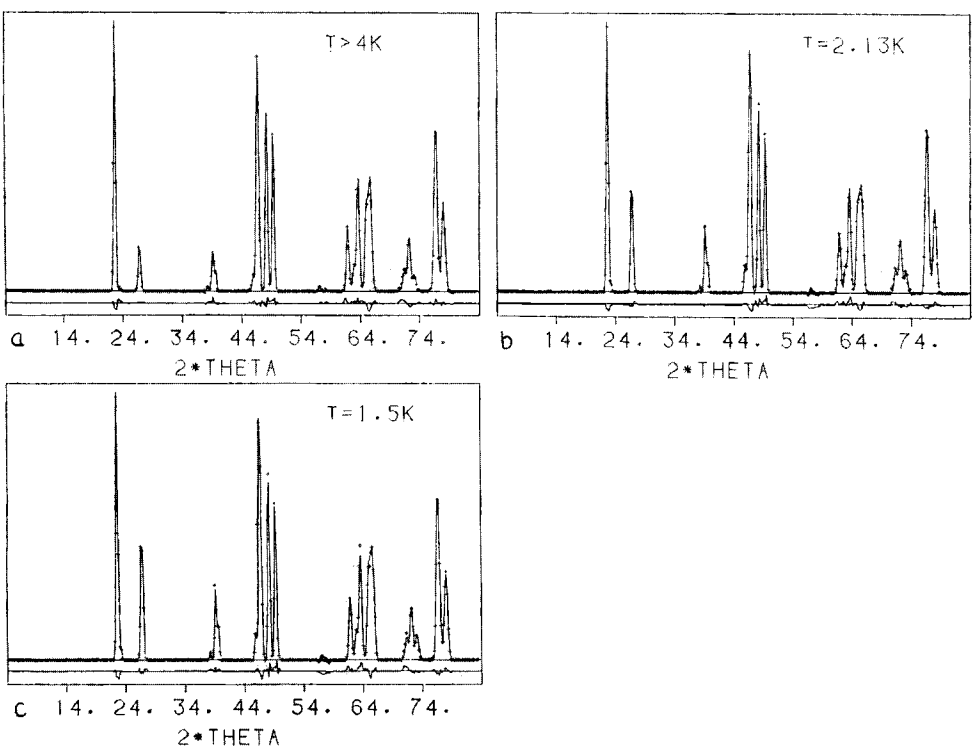

Fig. 2 Comparison between observed and calculated profiles of the Na_2NiCrF_7 pattern at 6 K (a), 2.13 K (b) and 1.5 K (c).

verified and corresponds to Fig. 1. The chains of trans corner-sharing Ni^{2+} octahedra, which run along [100], are linked together by isolated CrF_6 octahedra and form hexagonal tungsten bronze layers in the (011) and (01—1) planes. Fig. 2 gives the comparison between observed and calculated profiles.

2. Neutron thermo-diffractometry below T_c

The thermal variation of the integrated intensities of some significant peaks is shown in Fig. 3. Na_2NiCrF_7 orders magnetically below 4 K. As previously noted, the change in the magnetic intensities which occurs at 2 K, is clearly shown by arrows. In the range 4 to 2K, the intensities of some nuclear peaks

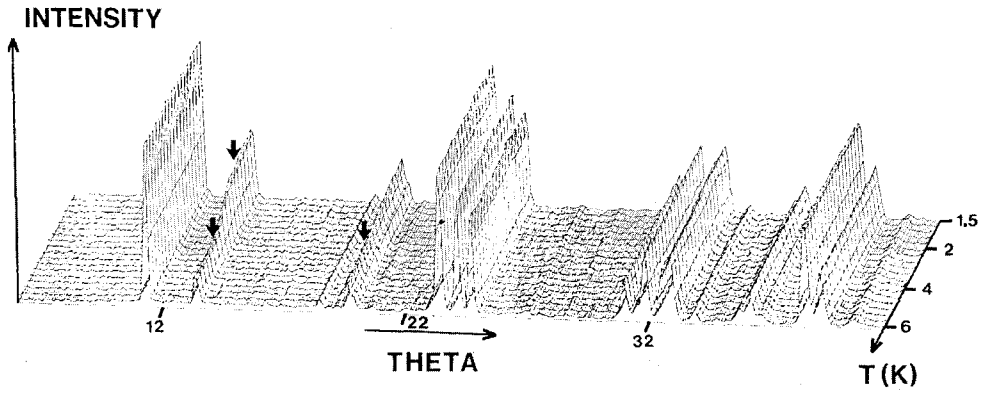

Fig. 3 Pseudo 3D plot of the patterns collected between 1.5 and 6 K. Arrows indicate the Curie temperature and the anomaly at 2 K.

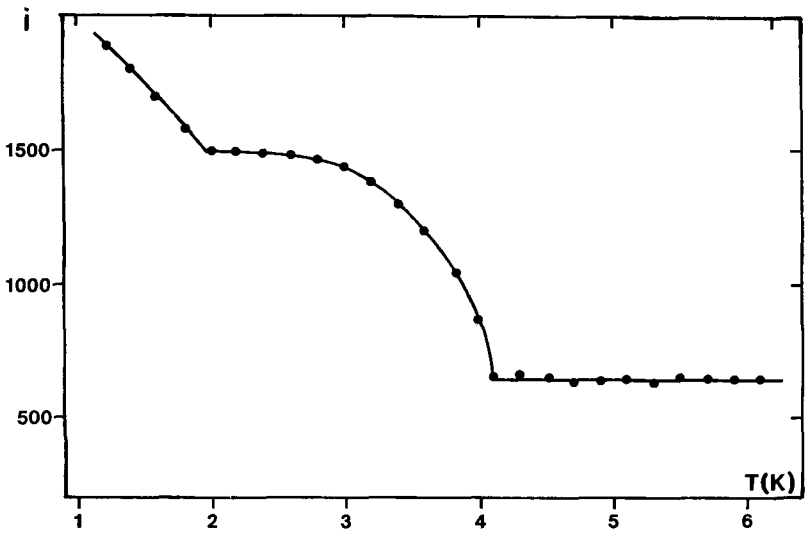

Fig. 4 Thermal variation of the intensity of the (101) reflection.

increases and no new magnetic intensities appear in the pattern: the magnetic and the nuclear cells are than identical. At 2 K, the magnetic intensities of some magnetic peaks abruptly increase (Fig. 4), whereas some others are not affected. A detailed study of the magnetic structure at 2.13 and 1.5 K was then undertaken to investigate this magnetic anomaly.

3. Magnetic structures

As already noted, at 1.5 and 2.13 K, no additional peaks appear in the pattern and therefore, the space group is considered to remain Imma above and below 2 K. The magnetic structure can be sought using macroscopic BERTAUT's theory [23]. $\tilde{2}_x$, $\tilde{2}_y$, -1 and I will be considered as the four independant symmetry elements. If R_i and S_i (i = 1,4) are the magnetic moments of Ni^{2+} and Cr^{3+} corresponding to the atomic coordinates reported in Table 3, it is possible to define in each sublattice four linear combinations of the moments:

$$F = M_1 + M_2 + M_3 + M_4$$
$$G = M_1 - M_2 + M_3 - M_4$$
$$C = M_1 + M_2 - M_3 - M_4$$
$$A = M_1 - M_2 - M_3 + M_4$$

Table 3 Atomic coordinates of the spins of Ni^{2+} (R_i) and Cr^{3+} (S_i) and corresponding magnetic modes in space group Imma

	Ni^{2+}					Cr^{3+}					
R_1	1/4	1/4	1/4		S_1	0	0	1/2			
R_2	3/4	1/4	1/4		S_2	0	1/2	1/2			
R_3	3/4	3/4	3/4		S_3	1/2	1/2	0			
R_4	1/4	3/4	3/4		S_4	1/2	0	0			
	mode										
	2_x	2_y	-1	I							
$\Gamma 1$	+	+	+	+		.	G_y	.		G_x	. .
$\Gamma 2$	−	+	+	+		.	F_y	.		.	F_y G_z
$\Gamma 3$	+	−	+	+		F_x	.	G_z		F_x	. .
$\Gamma 4$	−	−	+	+		G_x	.	F_z		.	G_y F_z
$\Gamma 5$	+	+	−	+		.	.	.		.	. .
$\Gamma 6$	−	+	−	+		.	.	.		.	. .
$\Gamma 7$	+	−	−	+		.	.	.		.	. .
$\Gamma 8$	−	−	−	+		.	.	.		.	. .
$\Gamma 9$	+	+	+	−		.	.	.		C_x	. .
$\Gamma 10$	−	+	+	−		.	.	.		.	A_y C_z
$\Gamma 11$	+	−	+	−		.	.	.		A_x	. .
$\Gamma 12$	−	−	+	−		.	.	.		.	C_y A_z
$\Gamma 13$	+	+	−	−		.	C_y	.		.	. .
$\Gamma 14$	−	+	−	−		.	A_y	.		.	. .
$\Gamma 15$	+	−	−	−		A_x	.	C_z		.	. .
$\Gamma 16$	−	−	−	−		C_x	.	A_z		.	. .

which represent the ferromagnetic and antiferromagnetic modes of coupling. The base vectors, in the irreducible representation of space group Imma, lead (Table 3) to sixteen modes. Only the modes Γ_1 to Γ_4 can describe the ferrimagnetic behaviour of Na_2NiCrF_7.

The best fit ($R_{mag} = 0.061$ at 2.13 K (Fig. 2b), $R_{mag} = 0.054$ at 1.5 K (Fig. 2c)) between observed and calculed magnetic intensities (the list of observed and calculed magnetic intensities can be obtained on request to G. F.) are obtained for the Γ_4 mode with signs $+G_x$, $+F_z$ for Ni^{2+} components and $-G_y$, $-F_z$ for Cr^{3+}. Other combinations of signs lead to an increase of the R factor. The corresponding value of the components of the magnetic moments are listed in Table 4.

Table 4 Refined values of the components of the magnetic moments at T = 2.13 K and 1.5 K in the mode Γ_4. Standard deviations are given in parentheses

	Ni^{2+}				Cr^{3+}			
T (K)	R_x	R_y	R_z	$\|R\|$	S_x	S_y	S_z	$\|S\|$
2.13	1.63		0.21	1.65		−0.08	−1.84	1.84
	(0.11)		(0.09)			(0.05)	(0.12)	
1.50	1.70		0.42	1.75		0.03	−2.22	2.22
	(0.09)		(0.08)			(0.05)	(0.10)	

T (K)	R_p	R_{wp}	R_{nuc}	R_{mag}
2.13	5.28	5.32	3.95	6.08
1.50	5.45	5.54	3.72	5.44

The two magnetic sublattices of Ni^{2+} and Cr^{3+} are quasiorthogonal (Fig. 1), the angle between $\mu_{Ni}{}^{2+}$ and $\mu_{Cr}{}^{3+}$ being 103.9° at 1.5 K (97.3° at 2.13 K). Magnetic dipolar energy calculations carried out in the real space inside a sphere of 50 Å radius show that $Ni^{2+}-Cr^{3+}$ dipolar coupling (Table 5) is predominant but negligible towards exchange energy.

Table 5 Partial magnetic dipolar energies in Na_2NiCrF_7. $E_{M_1M_2}$ represents the energy of the M_1 ion in a M_2 surrounding

M_1-M_2	$E_{M_1M_2}$ (J · mole^{-1})	
	T = 2.13 K	T = 1.5 K
$Ni^{2+}-Ni^{2+}$	0.249	0.277
$Ni^{2+}-Cr^{3+}$	−0.185	−0.258
$Ni^{2+}-Cr^{3+}+Ni^{2+}$	0.064	0.020
$Cr^{3+}-Cr^{3+}$	−0.001	−0.002
$Cr^{3+}-Ni^{2+}$	−0.185	−0.258
$Cr^{3+}-Cr^{3+}+Ni^{2+}$	−0.186	−0.259

For the Ni^{2+} sublattice, the spins are mainly coupled antiferromagnetically along [1 0 0] with however a canting along [0 0 1] due to a ferromagnetic component in this direction. The canting angle (7° at 2.13 K and 24° at 1.5 K) increases when the temperature is lowered. This situation must be compared to the behaviour in the weberite Na_2NiAlF_7 [25] which exhibit the same arrangement for the spins, mainly along [1 0 0], the canting angle being 40°. Moreover, the moments are close to the saturation at 2 K and the variation between 2 and 1.5 K is very weak.

The case of Cr^{3+} is different: whatever the temperature, the spins in this sublattice are antiferromagnetic along [001]. At 2 K, the moment is far from the saturation and increases in the range 2 —1.5 K. At this temperature, the saturation is not yet reached. The refinement of the magnetic structure at all temperatures recorded during the thermodiffractometric study clearly shows up the different thermal evolutions of the magnetic moments of Ni^{2+} and Cr^{3+}. It is responsible for the anomaly at 2 K, which does not correspond to a magnetic phase transition.

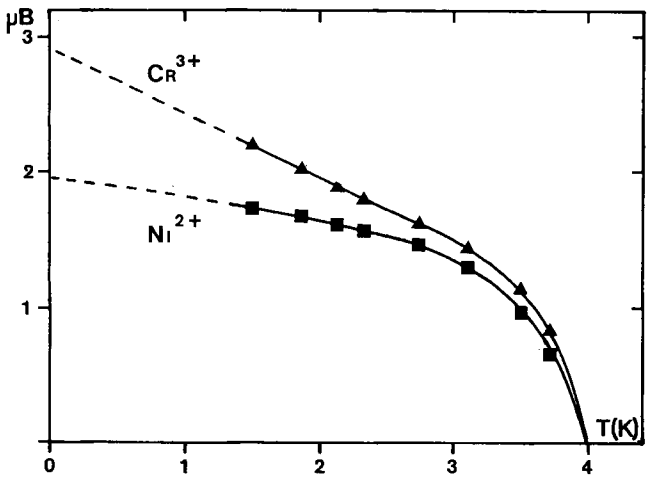

Fig. 5 Thermal variation of the moments of Ni^{2+} and Cr^{3+} below T_c.

This situation, which was already encountered for $NaMnFeF_6$ [26], differs from the cases of Na_2NiFeF_7 and the inverse weberite $Fe_2F_5(H_2O)_2$. These two compounds exhibit the same type of anomaly in the thermal variation of the intensities behaviour, but the reasons are different. For Na_2NiFeF_7, the accident at 55 K corresponds to a small reorientation of both Fe^{3+} and Ni^{2+} spins rather than a magnetic phase transition. For $Fe_2F_5(H_2O)_2$, below the accident at 26 K, a new magnetic reflection appears and induces a change in the magnetic space group. In this latter case, the two magnetic structures are very different and the anomaly corresponds to a complete change in the spin orientations. At $T > 26$ K, the anisotropy of Fe^{2+} governs the magnetic structure and obliges Fe^{3+} spins to adopt a parallel disposition. At $T < 26$ K, the antiferromagnetic coupling between Fe^{3+} becomes predominant and leads to a canted star structure.

Conclusion

These results clearly show that, when a series of isostructural magnetic compounds exhibits a frustrating topology, the frustrated magnetic structure strongly depends on the disparity of superexchange interactions. When M^{3+} is diamagnetic (i. e. Na_2NiAlF_7) [25], the frustration is suppressed and leads to a 1 D magnetic behaviour: the chains of Ni^{2+} are coupled antiferromagnetically ($T_N = 11$ K).

When M^{3+} is paramagnetic with $J_{M^{3+}-M^{2+}} < J_{M^{2+}-M^{2+}}$ (i. e. Na_2NiCrF_7), the Neel temperature is lowered ($T_N = 4$ K) the antiferromagnetic superexchange coupling between M^{2+} ions governs the structure. Ni^{2+} spins remain antiferromagnetic, whereas Cr^{3+} spins, weakly coupled to Ni^{2+} have some difficulties to saturate and adopt an orthogonal disposition towards the direction of Ni^{2+} moments. Finally, with a paramagnetic M^{3+} ion (Fe^{3+}) corresponding to $J_{M^{3+}-M^{2+}} > J_{M^{2+}-M^{2+}}$ (i. e. Na_2NiFeF_7 $T_c = 88$ K) (7,22), the $M^{2+}-M^{3+}$ interactions dominate and lead to a frustration of the antiferromagnetic coupling of Ni^{2+} spins which are obliged to adopt a parallel arrangement.

References

[1] FEREY, G.; DE PAPE, R.; BOUCHER, B.: Acta Crystallogr. **B 34** (1977) 1084.
[2] FEREY, G.; LEBLANC, M.; DE PAPE, R.; PANNETIER, J.: Solid State Commun. **53** (1985) 559.
[3] FEREY, G.; LEBLANC, M.; DE PAPE, R.; PANNETIER, J.: "Spin frustration problems in fluorides", in "Inorganic Fluorides: Chemistry and Physics", (Edited by P. HAGENMULLER), Academic Press, (1985) 395.
[4] LALIGANT, Y.; LEBLANC, M.; PANNETIER, J.; FEREY, G.: J. Phys. C, Solid State Phys. **19** (1986) 1081.
[5] LEBLANC, M.; PANNETIER, J.; DE PAPE, R.; FEREY, G.: Solid State Commun. **58** (1986) 171.
[6] LALIGANT, Y.; PANNETIER, J.; FEREY, G.: J. Solid State Chem., to appear in **67** (1987).
[7] LALIGANT, Y.; CALAGE, Y.; HEGER, G.; PANNETIER, J.; FEREY, G.: J. Solid State Chem. (submitted).
[8] FEREY, G.; DE PAPE, R.; LEBLANC, M.; PANNETIER, J.: Rev. Chim. Miner. **23** (1985) 474.
[9] LACORRE, P.; PANNETIER, J.; FEREY, G.: J. Magn. Magn. Mat. **66** (1987) 213.
[10] LACORRE, P.; LEBLANC, M.; PANNETIER, J.; FEREY, G.: J. Magn. Magn. Mat. **66** (1987) 219.
[11] BYSTROM, A.: Ark. Khem. Miner. Geol. **18B** (1944) 10.
[12] GIUSEPPETTI, G.; TADINI, C.: Tschermaks Miner. Petr. Mitt. **25** (1978) 57.
[13] HAEGELE, R.; VERSCHAREN, W.; BABEL, D.; DANCE, J. M.; TRESSAUD, A.: J. Solid State Chem. **24** (1978) 77.
[14] KNOP, O.; CAMERON, T. S.; JOCHEM, K.: J. Solid State Chem. **43** (1982) 213.
[15] HEGER, G.; VIEBAHN-HANSLER, R.: Solid State Commun. **11** (1972) 1119.
[16] TRESSAUD, A.; DANCE, J. M.; PORTIER, J.; HAGENMULLER, P.: Mat. Res. Bull. **9** (1974) 1219.
[17] HEGER, G.: Private communication.
[18] RIETVELD, H. M.: J. Appl. Crystallogr. **2** (1969) 65.
[19] HEWAT, A. W.: Acta Crystallogr. **A 35** (1979) 248.
[20] KOESTER, L.; RAUCH, H.: IAEA Contract 2517/RB (1981).
[21] WATSON, R. E.; FREEMAN, J.: Acta Crystallogr. **14** (1961) 27.
[22] WOLFERS, P.: Program "INTEGR", unpublished (1975).
[23] BERTAUT, E. F.: in Magnetism III, Rado and Shull Ed. (1963) 149.
[24] SHANNON, R. D.: Acta Crystallogr. **A 32** (1976) 751.
[25] HEGER, G.: Int. J. Magn. **5** (1973) 119.
[26] TAMINE, M.; CALAGE, Y.; LEBLANC, M.; FEREY, G.; VARRET, F.: Hyperfine Interactions **28** (1986) 529.

Bei der Redaktion eingegangen am 12. März 1987.

Anschr. d. Verf.: Prof. G. FEREY, Laboratoire des Fluorures, UA CNRS 449, Faculté des Sciences, F-72041 Le Mans Cedex